

**BNL Brookhaven National Laboratory
RHIC Accelerator Physics Group**

RHIC/AP/98-156

ARTUS: A Rhic TUne monitor System

**P. Cameron, R. Connolly, A. Drees,
T. Ryan, H. Schmickler^a, T. Shea, D. Trbojevic**

Abstract

The betatron tunes and related parameters like chromaticity and coupling have to be measured in RHIC from its first day of commissioning. This report describes various measurement techniques and their possible realizations. In general the beams must be excited externally due to the absence of inherent oscillations with significant amplitude. External excitation causes emittance growth which have to be limited in magnitude in particular on the operational beams for luminosity production.

July 1, 1998

^a CERN, SL Division

1 Introduction

The knowledge of the betatron tunes will be very important both for the routine operation of RHIC as well as for specific machine studies.

The fractional part q of the tune, which is desirable to be known much better than the width of the betatron line (i.e. better than 10^{-3}), can be measured using one single BPM only. For this the amplitude of the beam oscillation at one specific location has to be sampled for many turns. However, it is most likely that the oscillation amplitude which is beam inherent is too small. In this case it will either be necessary to stimulate the oscillation externally or improve the BPM resolution significantly. The external stimulation of oscillation will be done using a device which will be referred to as a **kicker**. Separate kickers have to be provided for both the horizontal and vertical plane and for the two rings. Although the basic purpose of ARTUS will be the measurement of the tunes the potential for diagnostics is much higher. The following machine experiments or measurements can be imagined:

- Measurement of the machine chromaticities, and even its derivative within the momentum acceptance of the machine.
- Measurement of the strength of the betatron coupling between the horizontal and vertical planes.
- Measurement of the local value of the β -function in a quadrupole from variation of its strength. This is of particular importance for the strong focusing quadrupoles of the experimental insertions.
- Measurement of the transverse impedance by measuring the tunes as a function of the beam currents.
- Observation of beam-beam modes, whose frequency splitting will yield information on the tune-shift parameters and can be used for luminosity optimization.

This report is structured in the following way:

1. Different measurement aims are discussed. Particular weight is given to the relative importance of various measurement techniques, the obtainable precision, and resulting emittance blow-up. Priority is given to those techniques, which have to be present at "Day 1" for the commissioning of the machine.
2. A list of hardware specifications for kickers and the tune system BPMs is derived and discussed in appendix B.1 and B.2
3. Faced with potential beam losses in super-conducting magnets and with quite high energy ramping rates the control of the betatron tunes, i.e. their measurement and eventual feedback or at least feed forward on magnetic elements will be an important issue. At a ramping rate of up to 1.3 GeV/s (AU) and 3.2 GeV/s (p) respectively, a tune monitoring update rate of about 1 Hz would allow one measurement per

GeV for gold and one measurement per 3 GeV for protons. The above measurement bandwidth of 1 Hz seems to be a good compromise between time resolution and emittance growth. A comprehensive summary of tools available for diagnostics and control of the time evolution of beam parameters can be found in [1]. The issue of tune control at RHIC leaves the scope of this report.

2 Measurement Methods

The following complementary methods are discussed:

1. Single kick beam excitation and spectral analysis,
2. Random noise excitation and spectral analysis,
3. Measurements of the whole beam transfer function (frequency sweeps of the beam exciter),
4. Resonant kicker excitation within a phase-locked loop for tune tracking,

The applicability of these methods differs considering the technical realization, required accuracies, conditions of the beam and the measurement time.

2.1 Decoherence of Betatron Oscillations

As a basis for the following calculations the expected decoherence times are listed depending on the operating conditions of RHIC:

| | | σ_p/p | $m(1/2)$ | $m(1/e)$ | Δq |
|----|-----------|---------------------|----------|----------|------------|
| AU | injection | $4.7 \cdot 10^{-4}$ | 133 | 160 | 0.001 |
| | | $7.4 \cdot 10^{-4}$ | 84 | 101 | 0.002 |
| | storage | $4.2 \cdot 10^{-4}$ | 226 | 268 | 0.001 |
| | | $6.4 \cdot 10^{-4}$ | 148 | 176 | 0.001 |
| p | injection | $5.1 \cdot 10^{-4}$ | 124 | 147 | 0.001 |
| | | $3.4 \cdot 10^{-4}$ | 279 | 331 | 0.0005 |

Table 1: *The decoherence time given in numbers of turns m and the approximate tune spread Δq for different operation modes.*

A bunch which is initially displaced by a certain arbitrary amplitude rotates in phase space with the betatron frequency around the origin $x = x' = 0$. With the increasing number of rotations the distribution spreads in transverse phase space until the entire annular region is populated and the particles are uniformly distributed around the origin. At this time the coherent signal disappears. Considering Gaussian shaped bunches and an initial displacement of x_0 the mean displacement \hat{x} after m turns is [2]:

$$\hat{x} = x_0 \exp \left[-0.5 \left(2\pi m \xi \frac{\sigma_p}{p} \right)^2 \right]. \quad (1)$$

The design values for the RHIC chromaticity ξ and energy spread $\frac{\sigma_p}{p}$ can be found in table 4. Given these values the number of turns to reduce the signal by 50% and to 1/e are listed in table 1.

2.2 Single Kick Excitation

Assuming a minimum necessary signal to noise ratio of 20 dB and a rms noise of 50 μm in the BPM used for tune measurements a single kick resulting in an initial amplitude of 500 μm would be needed for the tune measurement system.

The emittance growth of a single kick excitation can be evaluated for the various machine conditions and beam energies using the following formula [3]:

$$\sigma^2 = \sigma_0^2 + \frac{1}{2}(\beta^2 \Delta x'^2), \quad (2)$$

where σ corresponds to the beam size after a kick for tune measurements and σ_0 to the original beam size. Table 2 gives the initial beam oscillation amplitude after a single kick and the resulting emittance growth. At injection the required 500 μm can be achieved, whereas at storage energy only about 20% of the required amplitudes can be generated. However, the rms amplitude over twice the decoherence time amounts to about 40% of the initial amplitude. In all cases the emittance growth is acceptable, if not negligible. The lack of oscillation amplitude at storage energy leads to the next excitation mode. Table 2 summarizes the results for AU and p+ beams. The amplitude is calculated according to equation 6.

| | | Θ | β -ampl. | rms | $\Delta\epsilon/\epsilon$ (%) | |
|----|------|---------------------|-------------------|-------------------|-------------------------------|-------|
| | | (μrad) | (μm) | (μm) | hor. | vert. |
| AU | inj. | 11.4 | 775 | 340 | 1.6 | 0.7 |
| | sto. | 1.3 | 90 | 40 | 0.1 | < 0.1 |
| p | inj. | 11.0 | 750 | 330 | 1.9 | 0.8 |
| | sto. | 1.2 | 80 | 35 | 0.2 | 0.1 |

Table 2: *Emittance blow up after a single kick Θ for AU and p beams at injection and storage energies for a $\beta^* = 10$ m. See the Appendix for kicker parameters (B.1) and beta values at the BPMs (B.2).*

2.3 Random Kick excitation

In this mode the whole spectrum can be obtained at once by a digital Fourier Transformation of the beam response to a broad band excitation. In practice the beam would be kicked with a noise source of a known spectrum and the beam response spectrum would be measured. The ratio of the two spectra is the desired beam transfer function. Since no time is dedicated to wait for the stabilization of the system this method is fast compared to the swept frequency measurement, but it has less good signal quality due to the random nature of the excitation. In any case this method leads to a larger oscillation amplitude

than a single kick and gives at least a good reading of the main betatron lines. In case of continuous excitations the emittance growth has to be calculated differently. Equation 3 needs the rms beam oscillation during the measurement and the measurement time as input parameters. Again the beam oscillation amplitude is expressed as the product of the detector resolution and the required signal to noise ratio. This way the results can be scaled for any given measurement precision and for potential improvements in the oscillation detector:

$$\frac{\delta\epsilon}{\epsilon_0} = \frac{(S/N \cdot x_{\text{noise}})^2}{\beta} \cdot \delta Q \cdot \frac{\Delta t}{T} \cdot \frac{1}{\epsilon_0}, \quad (3)$$

where ϵ_0 is the original emittance, δQ corresponds to 4 x the rms tune spread, T is the revolution period ($= 12.8 \mu\text{s}$), Δt is the time interval of the beam oscillation, S/N is the signal to noise ratio and x_{noise} represents the noise figure of the BPM. Table 3 summarizes the results from simulations [4]. These simulation point out an easy to achieve gain factor of more than 10 comparing single kick RMS amplitude and random kick RMS amplitude. The random noise excitation of the beams is made using the presently available hardware, i.e. a pulsed mono-polar power supply applied to the strip line kickers. The random nature of the excitation is obtained by not firing the power supply in 50% of the revolutions. Different excitation levels can be generated by properly choosing the duty cycle of excitations and pauses. A slow variation of the excitation levels (needed during energy ramping) can be achieved by varying the power supply voltage by a maximum of a factor 5. The table shows that the requested oscillation amplitude of $500 \mu\text{m}$ can be achieved at storage energies, but the price to pay is a significantly high emittance blow-up. In the long term the noise figure of the BPMs will improve with higher beam intensities and shorter bunches, such that good quality tune measurements will be possible with smaller oscillation amplitudes.

| U_{kicker} | | RMS ampl. | $\Delta\epsilon/\epsilon$ |
|---------------------|-----|-------------------|---------------------------|
| 3000 V | v,h | 900 μm | 100 % |
| 600 V | v,h | 180 μm | 4 % |

Table 3: *Emittance blow up for Au at storage for random kick excitation and a $\beta^* = 10 \text{ m}$ for two different kicker voltages in both planes. The beam oscillations were simulated over a period of 1000 turns.*

2.4 Frequency Sweeps

A variable sine-wave frequency is applied to the kicker. The frequency will be swept with a certain increment following a step function. The step width has to be smaller than the width of the resonances to be measured. Data will be acquired over a large number of

turns and be analyzed by a Harmonic Analyzer. After each step the procedure has to be paused for several signal decoherence times (i.e. order of ms) to let the system reach its new stable state before applying the algorithm. Hence the measuring time depends on the decoherence time, on the desired precision, and on the total frequency range to be scanned. This method yields a very precise measurement of the beam transfer function, but due to its long measurement time its main application will be machine studies. Presently the necessary hardware of a bipolar linear and pulsed power supply is not available.

2.5 Phase Locked Loop

Most tune measurements use the amplitude peak of the beam oscillation as signal for tune measurements. This is somewhat odd, since the amplitude information with "0-slope" at its maximum suffers much more from noise than the phase information, which has its maximum slope at the tune resonance. Phase Locked Loop Circuits instead make use of the phase slope. The beams are excited with a continuous sine wave. By changing the frequency of the exciting oscillator an analog or digital circuit assures that the phase difference between excitation and beam motion is 90° . The tune measurement simply consists of a readout of the (filtered) frequency of the oscillator. In reality the design of such a PLL is more complicated, in particular the lock-in procedure and additional regulation circuits for constant amplitude of the beam oscillation. As the readout of the oscillator frequency can be made almost continuous a PLL circuit is the ideal tool for tracking the time evolution of the betatron tunes during machine transitions.

3 "Day 1" Functionality

To measure the fractional betatron tunes from the first day of operation on two scenarios have to be considered:

- **static** measurements at a stable energy setting (injection or storage) and
- **dynamic** measurements while the beam energy is changing (during the ramp).

Four BPMs, which are listed in appendix B.2, at locations with high betatron amplitudes are selected as ARTUS default devices. The tunes are obtained from an application of a fast Fourier transformation (FFT) to the collected data samples. Horizontal and vertical tune measurements are executed serially. At a static energy there are two different ways to trigger:

- trigger on event (injection only):
Bunches are injected with a certain displacement in the horizontal and vertical plane. This can be used for tune measurements without external stimulation provided the initial displacement was large enough to create an observable betatron oscillation at the BPM. A signal which marks the time of injection starts the data acquisition for

the selected BPMs providing four samples with data of 1024 turns each which are shipped to a central computer in the main control room (MCR).

- trigger on request:

A certain bunch is selected which will be stimulated externally by the transverse kickers. The kicker voltage can be varied between 600 and 3000 V in some steps. Data of 1024 turns from this bunch is collected by one BPM. More than one BPM is required at bad signal to noise conditions. This method is applicable at both injection and storage energies. With an initial amplitude of more than 500 μm at the BPM at injection the tune is easily obtainable. However, a RMS betatron oscillation of 40 μm at the BPM at storage is not sufficient to extract the tune - especially not at low beam currents. In the first year of operation low currents where the BPM resolution is around 50 μm are expected. Performing a series of kicks or selecting more sets of BPMs improves the tune resolution by \sqrt{N} where N is the number of kicks or BPMs respectively.

During the ramp (≥ 70 s) a sequence of kicks and acquisitions of 1024 turns for a certain bunch has to be performed at about 1 Hz. Since kicking with full power at injection causes a significant emittance blow-up if not a beam loss, the kicker voltages have to be adjusted during the ramp from the smallest value to full power at storage. Grouping the data samples according to their signal to noise ratio yields a set of tune measurements during the ramp.

4 Conclusion

Tune measurements are feasible in RHIC under all operating conditions with the standard BPM devices without further optimization of the currently published noise figures of the BPMs. A fast kicking device is foreseen for Day 1 achieving kick angles of at least 1 μrad at storage energies. With this device sufficient oscillation amplitudes can be built up at injection energies with single kicks, whereas at storage energies multiple random kicks are needed. The later method can lead to considerable emittance blow-up and hence the method has to be used with care. In any case any improvement on the front end electronics of the BPMs will yield better measurements or the same measurement quality with smaller emittance blow-up. The signal to noise ratio of the measurements will be good enough to further use the instrument for chromaticity and coupling diagnostics. More sophisticated tools like PLL tune tracking or measurements of the beam transfer function require for the beam excitation bipolar linear power supplies, which will be added to the machine at a later stage.

References

- [1] H. Schmickler, "Diagnostics and Control of the Time Evolution of Beam Parameters",

Proceedings of the Third European Workshop on Beam Diagnostics (DIPAC 97), Frascati, Italy, 12-14 October 1997.

- [2] R. Connolly, “Decoherence of Betatron Oscillations in RHIC”, AD/RHIC/RD-118 (1998).
- [3] Edwards, Syphers, “An Introduction of the Physics of High Energy Accelerators”, Wiley InterScience, 1993.
- [4] Roger Connolly, private communication.
- [5] J. Wei et al., “RHIC Longitudinal Parameter Revision”, RHIC/AP/145(1997).
- [6] W. Fischer et al., “Emittance Growth in RHIC during Injection”, RHIC/AP/112 (1997).
- [7] J. Xu et al., “The Transverse Damper System for RHIC”, Proceedings of the Particle Accelerator Conference in San Francisco, 1991.
- [8] P. Cameron, private communication.
- [9] D. Ciardullo, “Power Amplifier Selection For The RHIC Transverse Damper System”, RHIC beam instrumentation Website.
- [10] P. R. Cameron et al., “RHIC Beam Position Monitor Assemblies”, IEEE Proc. PAC 1993, p. 2328f (1993).
- [11] RHIC design report, section of beam instrumentation, April 1994.
- [12] P. R. Cameron et al., “RHIC Beam Position Monitor Characterization”, IEEE Proc. 1995 PAC.
- [13] William A. Ryan, private communication .

A Beam Parameters

Table 4 gives some relevant beam parameters of RHIC for reference throughout this report. The numbers are taken from [5]. The Laslett tune shifts (last row of table 4) are calculated using the following equation [6]:

$$\Delta Q_{x,y} = -\frac{Z^2 r_0 C N_b}{2(2\pi)^{3/2} A \beta^2 \gamma^3 \epsilon_{x,y} \sigma_L} . \quad (4)$$

B Hardware Requirements

B.1 Beam Excitation - The Kicker Magnet

Since the transverse beam motion is assumed to be mainly uncoupled, four separate systems are needed: one horizontal and one vertical for each of the two rings. Each kicker module is 2 m long, and contains 50 Ω strip lines for both horizontal and vertical planes. The strip lines

| symbol | quantity | unit | Gold | | protons | |
|-------------------------|-------------------------|-----------|-------------------------|---------------|-----------|---------------|
| | | | injection | store (begin) | injection | store (begin) |
| r_0 | classical proton radius | m | $1.5348 \cdot 10^{-18}$ | | | |
| C | RHIC circumference | m | 3833.845 | | | |
| T_{rev} | revolution time | μs | 12.8 | | | |
| N | number of bunches | | 60 | | | |
| N_b | bunch intensity | | 10^9 | | 10^{11} | |
| Z | atomic number | | 79 | | 1 | |
| A | mass number | | 197 | | 1 | |
| γ | relativistic factor | | 12.6 | 108.4 | 31.2 | 268.2 |
| E_0 | kin. energy | GeV/u | 10.8 | 100 | 28.3 | 250.7 |
| $\epsilon_{x,y}$ | RMS emittance | μm | 0.132 | 0.023 | 0.107 | 0.012 |
| $\xi = p \frac{dq}{dp}$ | chromaticity | | -3 | 2 | -3 | 2 |
| σ_p/p | momentum spread | 10^{-4} | 4.7-7.4 | 4.2-6.4 | 5.1 | 3.4 |
| σ_L | RMS bunch length | m | 0.55-0.88 | 0.11-0.17 | 0.38-0.51 | 0.07-0.09 |
| $\Delta Q_{x,y}$ | tune shift | | 0.031 | 0.001 | 0.013 | 0.001 |

Table 4: RHIC longitudinal parameters for AU and p^+ at injection and storage.

subtend 70° and the aperture is 7 cm. Each ring has 2 modules for a total of 4 m kicker length in either plane. The modules may be powered separately.

The kick angle Θ (in *rad*) received by an ion going through the kicker is given by [7]:

$$\Theta = \frac{Z e l_k V_k}{A E_0 \beta^2 d_k} \cdot \tau \eta \alpha, \quad (5)$$

where

Z atomic number

A mass number

e elementary charge

l_k length of the kicker, here 2x2 m

V_k voltage applied to one plate of strip-line

d_k plate separation

E_0 energy of ion beam

β relativistic velocity

τ transit time factor, here 1

η contribution factor from electric and magnetic field, here 2

α enhancement factor at center position, here 0.9

Equation 5 gives about the same results for gold ions and protons. Some values for two particular voltages at injection and storage energies are outlined in table 5. The kick is the same for both

| | V_k [V] | E_0 [GeV/u] | Θ [μ rad] |
|----|-----------|---------------|-----------------------|
| AU | 3000 | 10.8 | 11.4 |
| | 600 | 10.8 | 2.4 |
| | 3000 | 100 | 1.3 |
| | 600 | 100 | 0.24 |
| p | 3000 | 28.3 | 11.0 |
| | 600 | 28.3 | 2.4 |
| | 3000 | 250.7 | 1.2 |
| | 600 | 250.7 | 0.24 |

Table 5: Kick angles received by AU-ions and protons at various energies and kicker voltages.

the horizontal and vertical plane. The effect of such a kick translates into a beam offset given by:

$$\delta_{x,y} = \Theta \sqrt{\beta_{x,y}(s_0)\beta_{x,y}(s)} \sin \psi_{x,y}(s - s_0), \quad (6)$$

where $\beta_{x,y}(s_0)$ is the β -function at the location s_0 of the kicker and $\beta_{x,y}(s)$, $\psi_{x,y}(s)$ are the respective horizontal or vertical β -function and phase advance at location s . Table 6 lists the position of the installed kicker modules [8, 9] and the approximate beta-function and phase advance at these locations for various values of β^* . The beta-function of a device is computed at its longitudinal center position. In both rings kicker # 1 corresponds to the device which is closer to the interaction point.

| | | blue | | yellow | |
|--------------|----------------|----------|----------|----------|----------|
| | | kicker 2 | kicker 1 | kicker 1 | kicker 2 |
| s | | 2490.8 | 2492.8 | 2619.1 | 2621.1 |
| $\beta^*=10$ | β_x [m] | 31 | 35 | 35 | 31 |
| | β_y [m] | 17 | 14 | 14 | 17 |
| | ψ_x [rad] | 18.5 | 18.5 | 19.1 | 19.1 |
| | ψ_y [rad] | 19.0 | 19.0 | 19.9 | 19.9 |
| | α_x | -1.0 | -1.1 | 1.1 | 1.0 |
| | α_y | 0.7 | 0.5 | -0.5 | 0.7 |

Table 6: Position of the transverse kickers in RHIC with approximate betatron amplitude and phase advance relative to 6 o'clock.

B.2 Oscillation Observation - The BPM

The beam position monitors are realized by short circuited strip transmission lines. Table 7 summarizes the design parameters [10]. Each of the two rings accommodates 234 BPM devices [11] plus 12 monitors which are shared between the two rings since they are located in the Interaction Regions (IR) at the inner edges of the DX magnets. The DX magnets are the dipoles where the two separated vacuum chambers merge and re-separate again. The 174 single plane

| | |
|-----------------------|--|
| aperture | 69 mm (113 mm) |
| length | 23 cm |
| transfer function (*) | 0.7 (0.5) db/mm |
| impedance(*) | 50 ohm |
| subtended angle | 70 degree |
| resolution | between 2-3 μm and 50 μm |
| total device number | 480 |

Table 7: BPM design parameters and results from prototype measurements, which are marked with a (*). The BPM resolution depends on the bunch current and the gain settings.

detectors per ring are mounted on the sextupole end of the Corrector-Quadrupole-Sextupole package. A total of 72 monitors are dual plane devices allowing a simultaneous measurement of vertical and horizontal beam displacements. This leads to a sample of 161 BPM signals per ring available for either plane. Two (dual plane) BPMs out of the total of 480 are of particular

| | BPM (blue) | BPM (yellow) |
|-----------|------------|--------------|
| s | 2503.1 m | 2608.7 m |
| β_x | 66 m | 66 m |
| β_y | 13 m | 13 m |

Table 8: Location and approximate betatron function of the movable BPMs close to the interaction point at 2 o'clock (BRAHMS) for $\beta^* = 10$ m.

interest because they are movable within about 1 cm. These two or any other BPMs could be equipped with a modified readout electronics enabling a higher resolution in the order of 1 μm . This future upgrade is not foreseen for “Day 1”. However, for commissioning it is intended to

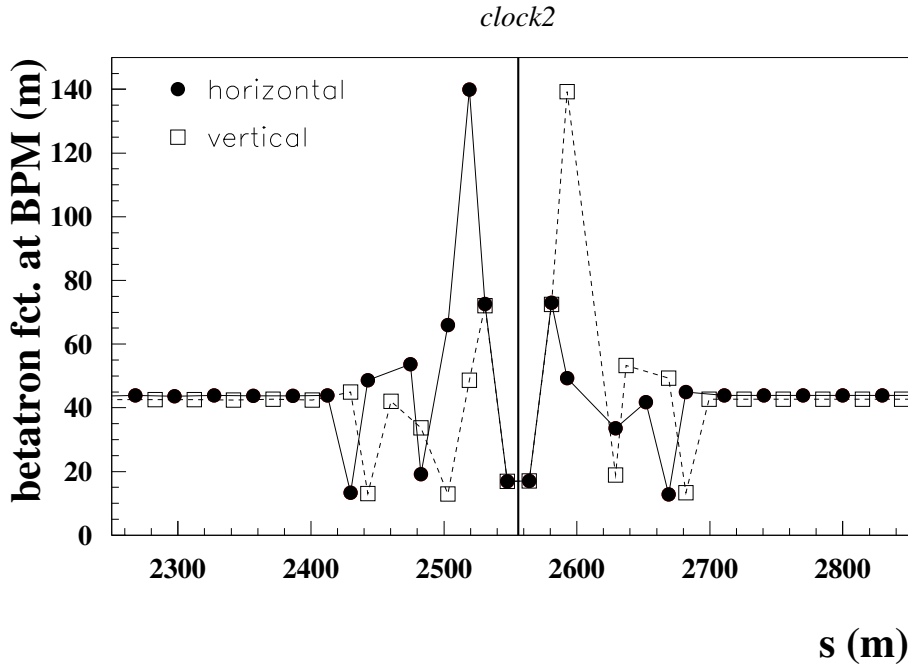


Figure 1: Vertical and horizontal betatron amplitude as a function of the BPM position around 2 o'clock in the BLUE ring at injection.

convert one BPM per ring into a resonant device with a high Q-value and a significant improved resolution.

Table 8 lists the position of the movable BPMs and the corresponding values of the betatron function. However, any BPM at a location with large betatron amplitude is convenient to be used for the tune meter. Candidates are in particular 8 BPMs located in the 2 o'clock and 6 o'clock area respectively close to the Q3 quadrupoles. Their prominent position is emphasized in figure 1. The selected BPMs have an enlarged aperture of 11.3 cm. Table 9 lists their position and properties. However, the noise figure of these large aperture BPMs with a smaller transfer function increases by a factor of $0.7/0.5 \simeq 1.4$ (see table 7) compared to the standard devices. The betatron amplitudes at the BPMs in the 2 o'clock are the same at injection and storage since the β^* does not change at 2 o'clock while at 6 o'clock it is squeezed to 1 m. Therefore the BPMs in the 6 o'clock area are most suitable to be used at storage once RHIC achieves the small β^* values. However, kick amplitudes given in this report refer to the 2 o'clock BPMs in table 9.

| ring | β^* (m) | sidewide name | plane | s (m) | $\beta_{x,y}$ (m) | $\psi_{x,y}$ (s) |
|--------|---------------|---------------|-------|--------|-------------------|------------------|
| blue | 10 | bpm.bi1-bh3.1 | x | 2519.0 | 139.9 | 18.6 |
| | | bpm.bo2-bv3 | y | 2592.8 | 139.3 | 19.7 |
| | 1 | bpm.bi5-bh3 | x | 3796.9 | 1293.2 | 27.9 |
| | | bpm.bo6-bv3 | y | 36.9 | 1275.3 | 0.24 |
| yellow | 10 | bpm.yi2-bh3.1 | x | 2592.8 | 139.9 | 19.0 |
| | | bpm.yo1-bv3 | y | 2519.0 | 139.3 | 19.2 |
| | 1 | bpm.yi6-bh3 | x | 36.9 | 1293.2 | 0.21 |
| | | bpm.yo5-bv3 | y | 3796.9 | 1275.3 | 28.96 |

Table 9: Naming convention and betatron amplitudes around 2 o'clock and 6 o'clock for the BPMs which are most convenient for ARTUS at injection and storage.

The accuracy of the beam position measurement is required to be within 130 microns from the magnetic centers of the quadrupole and sextupole to the number displayed in the main control room (MCR). Two error sources contribute:

- displacement of the measured center of the quadrupole and sextupole field with respect to the electrical center of the BPM [12],
- errors in the electronics.

Adding these sources in quadrature leads to an upper limit of about 100 microns for each component. First results from prototype assemblies [10] and survey measurements [12] show that the required position tolerances are not only attained but the measurements fall even below this limit. The locations of the measured electrical centers relative to the cryostat fiducials have a sigma of less than 50 microns. While the mechanical tolerances do not vary, the electrical error changes with the beam intensity. Bunch intensities or charges per bunch respectively from 10^8 up to high values of about 10^{12} have been simulated [13]. The simulated beam positioned in the electrical center of the BPM. The RMS values of the position measurements as a function

of the beam intensity are shown in Fig. 2 for the three gain settings, 0 db, +20 and +40 db. Each data sample includes 1000 measurements. The requirement of a reasonably small error

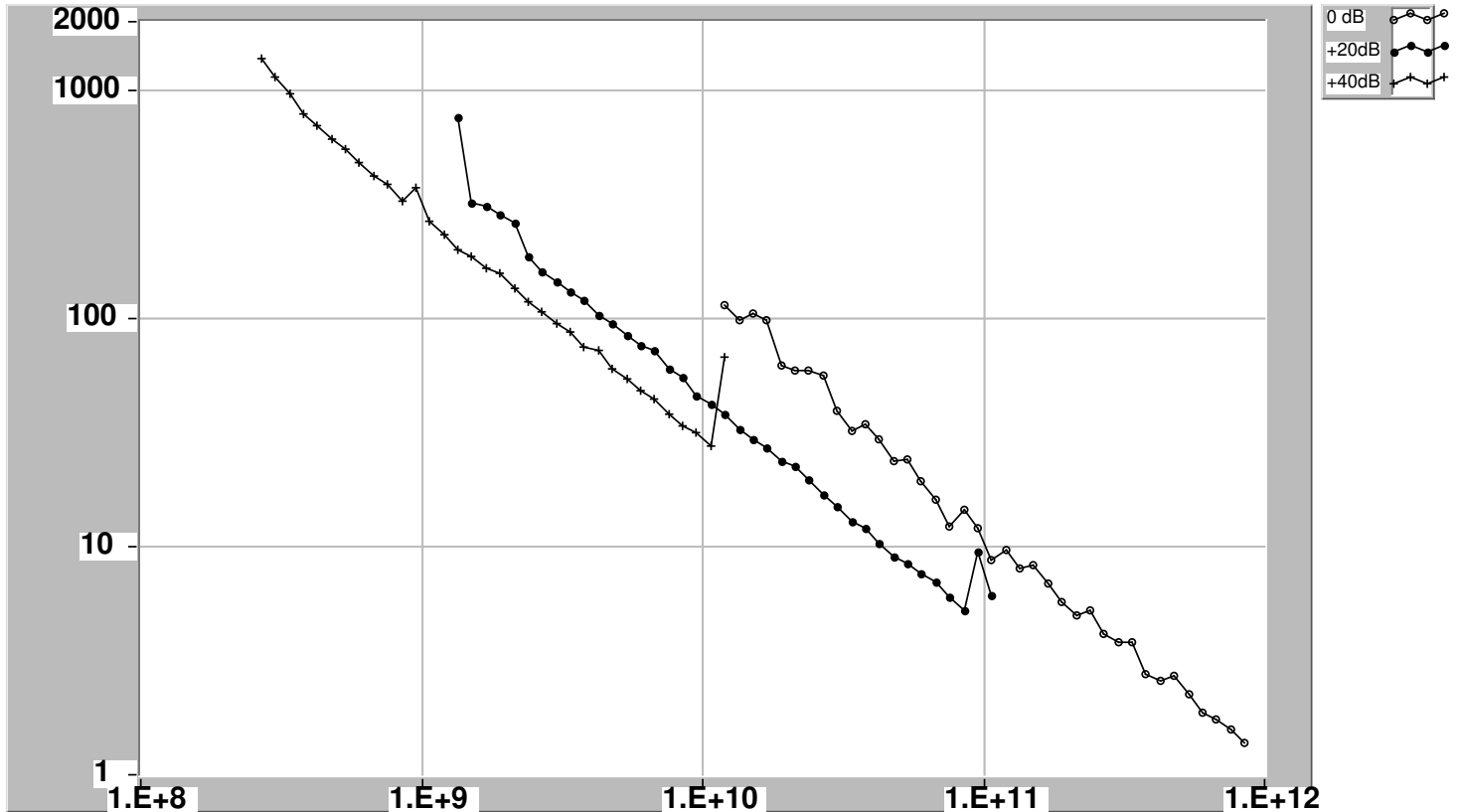


Figure 2: *RMS value of the BPM position measurement as a function of charges per bunch at a gain setting of 0 db (open circles), +20 db (closed circles) and +40 db (crosses).*

is accomplished for bunch intensities between 10^{10} and 10^{11} charges with a +20 db gain and for bunch currents from 10^{11} to about 10^{12} charges with a 0 db gain. The resolution of the BPMs within these ranges is in the order of the quoted $50 \mu\text{m}$ or better. The design AU bunch intensities are more than 10^9 ions per bunch what corresponds to about 10^{11} charges per bunch in the case of AU ions. Since the intensities during the first year of operation are expected to be smaller than that the +20 db setting is most likely to be used. However, in the startup period even smaller bunch currents might occur for various reasons. In this case a gain setting of +40 db has to be chosen. In order to ensure reliable position measurements with the required resolution an intensity above 8 or $9 \cdot 10^9$ charges per bunch is desirable.